Biophysical Journal
Article

Biophysical Society

# Protein Glycation by Glyoxal Promotes Amyloid Formation by Islet Amyloid Polypeptide

Yi-Hsuan Hsu,[1] Yun-Wen Chen,[2] Meng-Hsin Wu,[1] and Ling-Hsien Tu[1,*]
[1]Department of Chemistry, National Taiwan Normal University, Taipei, Taiwan and [2]Department of Pharmacology, College of Medicine, National Cheng Kung University, Tainan, Taiwan

ABSTRACT Protein glycation, also known as nonenzymatic glycosylation, is a spontaneous post-translational modification that would change the structure and stability of proteins or hormone peptides. Recent studies have indicated that glycation plays a role in type 2 diabetes (T2D) and neurodegenerative diseases. Over the last two decades, many types of advanced glycation end products (AGEs), formed through the reactions of an amino group of proteins with reducing sugars, have been identified and detected in vivo. However, the effect of glycation on protein aggregation has not been fully investigated. In this study, we aim to elucidate the impact of protein glycation on islet amyloid polypeptide (IAPP, also known as amylin) aggregation, which was strongly associated with T2D. We chemically synthesized glycated IAPP (AGE-IAPP) to mimic the consequence of this hormone peptide in a hyperglycemia (high blood sugar) environment. Our data revealed that AGE-IAPP formed amyloid faster than normal IAPP, and higher-molecular-weight AGE-IAPP oligomers were also observed in the early stage of aggregation. Circular dichroism spectra also indicated that AGE-IAPP exhibited faster conformational changes from random coil to its $\beta$-sheet fibrillar states. Moreover, AGE-IAPP can induce normal IAPP to expedite its aggregation process, and its fibrils can also act as templates to promote IAPP aggregation. AGE-IAPP, like normal IAPP, is capable of interacting with synthetic membranes and also exhibits cytotoxicity. Our studies demonstrated that glycation modification of IAPP promotes the amyloidogenic properties of IAPP, and it may play a role in accumulating additional amyloid during T2D progression.

SIGNIFICANCE Our investigation aims to provide a general model for islet amyloid polypeptide (IAPP) amyloid formation under hyperglycemia. In this study, we prove that protein glycation would change the amyloidogenicity of IAPP and expedite the process of IAPP aggregation. Glycated IAPP also exhibits its cytotoxicity.

## INTRODUCTION

Type 2 diabetes (T2D) is also characterized by the accumulation of pathological pancreatic islet amyloid fibrils, and islet amyloid polypeptide (IAPP) is the major component of the amyloid deposits. More than 95% of the patients suffering from diabetes are found to have amyloids in the islets of Langerhans (1–4). IAPP is a 37-residue, C-terminal amidated peptide hormone cosecreted with insulin from the secretory granules of the islet $\beta$ cells (5–8). The causal relationship between islet amyloid and T2D is not fully determined, but evidence has been found that IAPP oligomers are toxic to $\beta$ cells. We currently are unable to prevent its aggregation and save $\beta$-cell function and mass (9–11). The IAPP aggregation process was generally considered as a nucleation-dependent polymerization; as a result, fibril formation kinetics are typically shown in the form of a sigmoidal curve. Basically, there are three important stages: IAPP monomers show a concentration-dependent lag time during which no apparent aggregates were observed, followed by an elongation phase when enough IAPP oligomers were accumulated and served as seeds to induce rapid aggregation. In the end, aggregation reached a reaction plateau, in which the IAPP monomers are in equilibrium with amyloid fibrils. The seeds somehow can be seen as a template with special structural features to nucleate the formation of large IAPP aggregates. Therefore, the lag time can be significantly eliminated when a small portion of preformed fibrils are present in a pool of IAPP monomers (12). The structural characteristics of "toxic" IAPP oligomers have not yet been primarily defined because of their fast transformation. The amyloidogenicity of IAPP is

*Submitted November 13, 2018, and accepted for publication May 14, 2019.*
*Correspondence: litu@ntnu.edu.tw
Editor: David Eliezer.
https://doi.org/10.1016/j.bpj.2019.05.013

believed to be determined by certain amino-acid sequences. Residue modification or mutation on IAPP may affect its propensity to form $\beta$-sheet conformation. For example, rat IAPP only has six residues different from human IAPP, whereas rat IAPP does not form amyloid (13). The transgenic mice that carry the human IAPP gene do lead to amyloid formation in vivo (14). Although the details of interactions involved in the early stage of IAPP amyloid formation are not well understood, a number of mutational studies have shown that alterations on some of the amino-acid side chain would significantly accelerate or decelerate IAPP aggregation. Recently, deamidation, a kind of spontaneous nonenzymatic post-translational modification that causes the change of asparagine into a mixture of aspartic acid and isoaspartic acid, was discussed in modulating IAPP self-assembly (15,16). One of the study results shows that Asn 14 and Asn 21—but not Asn 22, Asn 31, and Asn 35—are key contributors to IAPP amyloid formation. Even a small portion of deamidated IAPP (N14D) is capable of inducing the aggregation of wild-type IAPP. A fragment of residues 20–29 was first considered as an amyloidogenic region because of the comparison of aggregation properties of rat and human IAPP (17,18). However, a number of mutations, including F15L and Y37L, occur outside of this region and show a different effect on the rate of IAPP aggregation (19). These all suggest that IAPP aggregation is very sensitive to residue change or post-translational modifications.

Protein glycation, a very different process from glycosylation, usually occurs between a free amino group of a protein and the carbonyl group of reducing sugars, such as fructose or glucose, and results in the permanent formation of advanced glycation end products (AGEs). This process, also called the Millard reaction, is a nonselective and nonenzymatic modification (20). In the past decades, the chemical structures of a variety of AGEs formed during this nonenzymatic type of glycosylation have been intensively studied and identified. Among these amino acids, the $\epsilon$-amino group of lysine and the guanidino group of arginine have been identified as the main targets of protein glycation (21,22). Among the AGEs, $N^{\epsilon}$-(carboxymethyl)-L-lysine, denoted as CML, is the most frequent modification found in glycated proteins (23). The formation of AGEs seems to promote the deposition of modified proteins because of gaining of further resistance to proteolytic degradation and removal processes. When blood sugar is increased, the chance of forming AGEs is greatly enhanced. Hence, these AGEs have been initially connected with diabetes (20). Later, it also has been proved to be involved in neurodegenerative diseases including Alzheimer's disease (AD) and Parkinson disease (24). Because different amyloidogenic proteins in amyloid deposits were found to be frequently glycated, a strong correlation is suggested between protein glycation and amyloidosis. However, glycation seems to cause different effects on protein aggregation (25–28). As for IAPP, a previous immunohistochemical study of pancreases from individuals with T2D has strongly suggested that IAPP is modified in amyloid deposits and AGEs colocalize with the presence of IAPP-derived islet amyloids in pancreatic islets, indicating that plasma IAPP may exist as a glycated form (29,30). In earlier study, Bucala and his co-workers first discussed the contribution of AGEs on islet amyloid formation. They prepared AGE-modified IAPP in vitro by incubating IAPP and glucose for 3 months at 37°C. The resulting protein aggregates showed better seeding efficiency than freshly dissolved IAPP and also exhibited higher cytotoxicity than control IAPP. These studies motivate us to carefully deduce the role of glycation in amyloid formation by IAPP from the view of a protein molecule.

## MATERIALS AND METHODS

### Peptide synthesis and purification

IAPP and AGE-IAPP were synthesized with a 0.05 mmol scale on a CEM Liberty Lite microwave-assisted peptide synthesizer (CEM, Matthews, NC) using Fmoc chemistry. A low loading of Rink Amide ProTide Resin (0.18 mmol/g; CEM) was used as a solid-phase support and to generate an amidated C-terminus after peptide cleavage. Diisopropylcarbodiimide was used in the activation of a carboxylic group of Fmoc-protected amino acids, and standard Fmoc reaction cycles were used. In addition, Fmoc-protected pseudoproline dipeptide derivatives were also incorporated at positions 8–9 and 27–28 to facilitate the synthesis (31). The $\beta$-branched residues, the residues which follow after the $\beta$-branched residues, all Arg, and all pseudoproline dipeptide derivatives were double-coupled to increase synthesis yield. By default, His was coupled at 50°C to minimize racemization. For AGE-IAPP synthesis, the only but also the last Lys residue was subsequently replaced by Fmoc-L-CML(OtBu) (Boc)-OH (N-$\alpha$-(9-Fluorenylmethyloxycarbonyl)-N-$\varepsilon$-t-butyloxycarbonyl-N-$\varepsilon$-(t-butoxycarbonylmethyl)-L-lysine; Iris Biotech, Marktredwitz Germany). Peptides were cleaved from the resin by standard trifluoroacetic acid methods; water, triisopropylsilane, and 3,6-dioxa-1,8-octanedithiol were used as scavengers (trifluoroacetic acid/$H_2O$/triisopropylsilane/3,6-dioxa-1,8-octanedithiol = 92.5:2.5:2.5:2.5). Crude peptides were partially treated with 20% acetic acid (v/v) and freeze-dried by several cycles to increase peptide solubility. Crude peptides were dissolved in oxidation solution, acetonitrile:$H_2O$ (1:1, v/v) with CLEAR-OX resin (Peptides International, Louisville, KY) to form the disulfide bond between Cys 2 and Cys 7. Peptides were purified by reverse-phase high-performance liquid chromatography using a Proto 300 C18 semipreparative column (Higgins Analytical, Mountain View, CA). A two-solution gradient was used: solution A consisted of 100% $H_2O$ and 0.045% HCl (v/v), and solution B consisted of 80% acetonitrile, 20% $H_2O$, and 0.045% HCl. The collected fractions were pooled and lyophilized. The peptide molecular weight was confirmed by low-resolution electrospray mass spectrometry (positive mode; AB SCIEX, Framingham, MA). For IAPP ($C_{165}H_{261}N_{51}O_{55}S_2$), calculated: 3903.28; found: *m/z* 977.45 $[M + 4H]^{4+}$, *m/z* 1302.73 $[M + 3H]^{3+}$, and *m/z* 1953.66 $[M + 2H]^{2+}$. For AGE-IAPP ($C_{167}H_{263}N_{51}O_{57}S_2$), calculated: 3961.2; found: *m/z* 991.80 $[M + 4H]^{4+}$, *m/z* 1321.84 $[M + 3H]^{3+}$, and *m/z* 1982.33 $[M + 2H]^{2+}$.

### Thioflavin-T assays

100 $\mu$g IAPP and AGE-IAPP protein powder were first treated with 100 $\mu$L hexafluoro-2-propanol for 5–6 h at room temperature and lyophilized. The resulting peptide powder was dissolved in 100 $\mu$L, 10 mM Tris buffer at pH 7.4 and centrifuged at 15,000 rpm for 10 min to remove preformed

aggregates. The solution supernatant was transferred into another microtube, and 10 $\mu$L of that was used to determine peptide concentration via BCA protein assay kit (Thermo Fisher Scientific, Waltham, MA). The peptide solution was prepared at a concentration of 32 $\mu$M with 32 $\mu$M thioflavin-T (ThT). ThT assays were performed at 25°C in a sealed 384-well nonbinding surface microplate (Corning, Corning, NY) without further agitation. Measurements were made using a SpectraMax M2 multimode microplate reader (Molecular Devices, San Jose, CA) with excitation at 430 nm and emission at 485 nm. The data were collected one time per hour, averaged from triplicate wells, and plotted as fluorescence versus time. For seeding experiments, the seeds were prepared by incubating 32 $\mu$M IAPP or AGE-IAPP in microtubes in a ThermoMixer (Eppendorf, Hamburg, Germany) with continuous shaking at 500 rpm for 4 days to form mature fibrils, and 10% of seeds (in monomeric unit) were added at the beginning of the reaction.

## Circular dichroism

Circular dichroism (CD) experiments were performed using a JASCO J-715 circular dichroism spectrometer (JASCO, Tokyo, Japan). The protein solutions prepared for CD experiments were similar to the samples for ThT assays, but peptides were incubated in microtubes in a ThermoMixer (Eppendorf), which shook at 500 rpm for 60 s/h. At desired time points, samples were transferred into a 1 mm pathlength quartz cell. Spectra were recorded from 198 to 260 at 1 nm intervals at 25°C. The data were averaged from 10 scans and corrected with background spectrum.

## Transmission electron microscopy

Transmission electron microscopy (TEM) was performed in the instrumentation center at National Taiwan University using a Hitachi H-7100 transmission electron microscope (Hitachi, Tokyo, Japan) with an accelerating voltage of 120 kV. 5 $\mu$L of peptide solution from the end of ThT assays was placed on a carbon-coated Formvar 300 mesh copper grid for 1 min and then negatively stained by incubation with 2% sodium phosphotungstate for another 1 min.

## Photoinduced cross-linking of unmodified protein

IAPP and AGE were prepared at 32 $\mu$M in 10 mM Tris buffer (pH 7.4) at 25°C. At the desired time, samples were cross-linked by adding 1 mM $Ru(bpy)_3^{2+}$ and 20 mM ammonium persulfate (APS) in 10 mM sodium phosphate (peptide/$Ru(bpy)_3^{2+}$/APS = 1:2:5) and illuminated with a 150 W incandescent light bulb for 5 s. The reaction was quenched by the addition of 4× sodium dodecyl sulfate (SDS) sample dye, and samples were separated by electrophoresis through a 13.5% Tris-tricine SDS polyacrylamide gel (SDS-PAGE). The gel was visualized by Western blot analysis with an antiamylin antibody (R10/99; Bio-Rad, Hercules, CA).

## Dye leakage assays

Lipids—1,2-dimyristoyl-*sn*-glycero-3-phosphocholine (DMPC) and 1,2-dimyristoyl-*sn*-glycero-3-phosphorylglycerol sodium salt (DMPG)—and cholesterol (3:1:1) were first dissolved in 100% chloroform in a 50-mL round-bottomed flask, and chloroform was evaporated with a stream of nitrogen gas to form lipid films. It was dried under a vacuum for 2–3 h to completely remove the residual organic solvent. The lipid film was rehydrated by adding 50 mM carboxyfluorescein in 20 mM Tris buffer with 100 mM NaCl (buffered to pH 7.4 by adding NaOH). The solution was vortexed several times until the lipids were fully dispersed. The multilamellar vesicles were then subjected to 10 freeze-thaw cycles and extruded 15 times through 2-stacked 100-nm pore size filters with an Avanti Mini-Extruder (Avanti Polar Lipids, Alabaster, AL). Nonencapsulated carboxyfluorescein was separated via size-exclusion chromatography using a PD-10 column (GE Healthcare, Chicago, IL) and eluted with 20 mM Tris buffer with 100 mM NaCl at pH 7.4. The phospholipid concentration was determined by phospholipid assay kit (colorimetric method; BioVision, Milpitas, CA). Another membrane vesicle containing 49 mol% 1-palmitoyl-2-oleoyl-glycero-3-phosphocholine (POPC), 21 mol% 1-palmitoyl-2-oleoyl-*sn*-glycero-3-phospho-L-serine (POPS), and 30 mol% cholesterol was also prepared in this study. Aliquots of IAPP or AGE-IAPP stock solutions were added into carboxyfluorescein-filled vesicles to reach the desired peptide/vesicle ratio (1:100). The final concentration of peptide for dye leakage experiments is 12 $\mu$M. The released dye fluorescence assay was monitored using an excitation wavelength of 492 nm and an emission wavelength of 517 nm after 8 h incubation at 25°C. The percent leakage of the dye is calculated as $100 \times (F_t - F_b)/(F_{max} - F_b)$, where $F_b$ represents the fluorescence intensity measured for vesicles with buffer and $F_{max}$ represents maximal fluorescence signal obtained after addition of 1% of Triton X-100 to induce complete dye leakage.

## Cell culture

Murine insulin-secreting MIN6 cells, passage 20–30, were maintained in Dulbecco's Modified Eagle's Medium (Gibco, Gaithersburg, MD) containing 25 mM glucose, 10% heat-inactivated fetal bovine serum (Gibco), 100 U/mL penicillin, 100 $\mu$g/mL streptomycin (Gibco), 10 mM HEPES (Gibco), 1 mM sodium pyruvate (Gibco), and 2 mM GlutaMax (Gibco) in a humidified atmosphere containing 95% air and 5% $CO_2$ at 37°C. Subculture and maintenance were performed as previously described (32). Cultured cells were passaged every 3–4 days.

## Cell viability assay

MIN6 cells were seeded in a 96-well plate ($8 \times 10^4$ cells/well) and cultured for 3 days before exposure to various concentrations of IAPP, AGE-IAPP, IAPP/AGE-IAPP = 1:1 for 4 and 24 h. After the indicated time, the media were removed and then added to 100 $\mu$L growth medium containing 10 $\mu$L Alamar Blue. After incubating for 4 h, the cell viability was quantified by measuring the absorbance of the solution at 570 and 600 nm wavelength.

# RESULTS AND DISCUSSION

## Protein glycation enhances the amyloidogenicity of IAPP

The primary sequences of IAPP and AGE-IAPP are both shown in Fig. 1. To access the impact of protein glycation on IAPP aggregation, we chemically synthesized AGE-IAPP by replacement of Lys1, the only Lys residue, with CML to mimic the consequence of protein glycation reaction. Protein glycation is a complex process and involves the formation of highly active dicarbonyl compounds, e.g., glyoxal, methylglyoxal, and 3-deoxyglucosone produced from the early stage of the Millard reaction (33). These active molecules would further react with an amino group of protein side chains to generate AGEs (34). In particular, CML is one of the well-characterized glyoxal-derived AGEs and the major product formed from the reaction of Lys with reducing sugars under physiological conditions (23). In the past, a number of studies were also conducted to explore the effect of protein glycation on protein aggregation. For

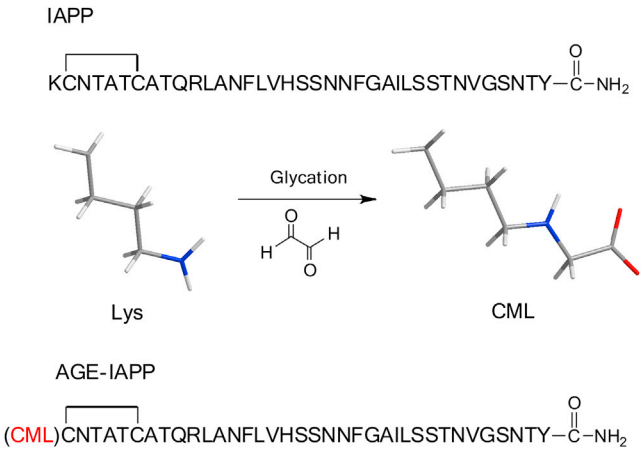


FIGURE 1 The primary sequence of IAPP and AGE-IAPP. The first amino acid of AGE-IAPP was mutated by CML and AGE-IAPP was used to study the effect of protein glycation on IAPP aggregation. Two peptides were chemically synthesized with amidated C-terminus and contain a disulfide bond between Cys2 and Cys7. To see this figure in color, go online.

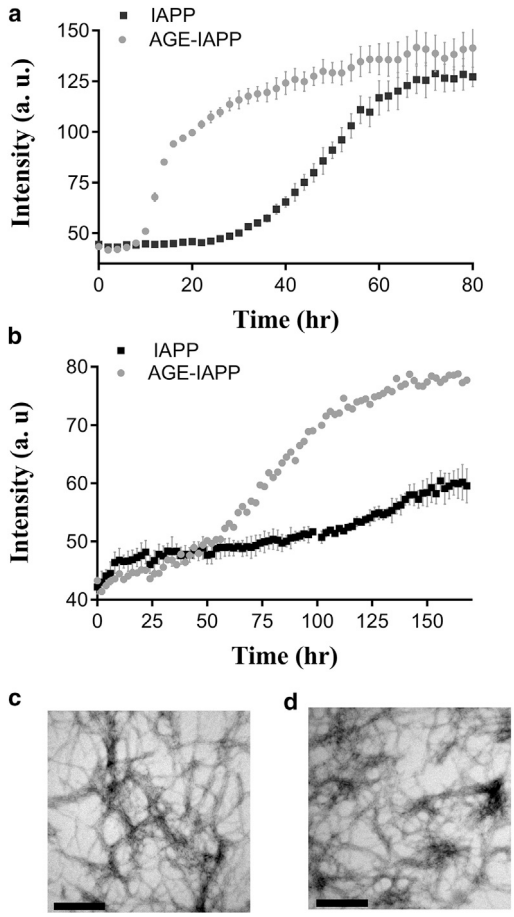


FIGURE 2 Glycation accelerates amyloid formation by IAPP. (*a*) ThT-assay-monitored kinetic experiments for 32 $\mu$M IAPP (*square*) and AGE-IAPP (*dots*) in 10 mM Tris buffer at pH 7.4 are shown. (*b*) ThT-assay-monitored kinetic experiments for 32 $\mu$M IAPP (*square*) and AGE-IAPP (*dots*) in 10 mM Tris buffer at pH 4.0 are shown. The kinetic experiments were done in triplicate. (*c*) TEM image of amyloid fibrils formed by IAPP is shown. (*d*) TEM image of amyloid fibrils formed by AGE-IAPP is shown. The scale bar represents 200 nm.

examples, modification of AD-related amyloidogenic peptide (A$\beta$) by AGEs has been shown to enhance peptide aggregation in vitro (35–37). D-ribose glycation of insulin prevents amyloid aggregation but produces cytotoxic species (38). AGE-modified IAPP aggregates can nucleate IAPP aggregation (29). In these studies, the glycated protein preparation was usually achieved through incubation of a high concentration of sugar with protein at 37°C in sterile conditions for weeks and even for months. IAPP aggregation is a spontaneous process in aqueous solution, and no extra agitation was needed to initiate the reaction. We are perhaps not able to prepare AGE-IAPP in nonaggregated form by similar approaches. Therefore, we chose to chemically synthesize glycated IAPP and study how this modification affects protein aggregation.

First of all, amyloid formation of both peptides was monitored by the conventionally used fluorescent dye ThT. ThT is a small molecule with benzothiazole structure, and the increase of fluorescence of ThT upon binding to aggregates makes it able to diagnose amyloid structure (39). Although ThT is not perfectly specific for amyloid, previous studies have successfully shown that it can be used to study IAPP aggregation, and the concentration used here does not alter the kinetics of IAPP. The data collected for IAPP show a typical three stages as previously described. Under the conditions used in this study, IAPP at 32 $\mu$M exhibited a lag time of 30 h, whereas the ThT fluorescence intensity of AGE-IAPP started to increase after 10 h incubation, suggesting glycation modulated IAPP amyloid formation (Fig. 2 *a*). Modification of Lys with CML accelerated amyloid formation, and the final ThT intensity of both peptides after 80 h incubation was relatively similar. IAPP is one of the naturally occurring amyloidogenic polypeptides; besides residue changes, the rate of its aggregation is also sensitive to some small changes such as solution condition, including ion composition, ionic strength, and pH. For example, studies have shown that increase of salt concentration leads to a significant reduction of the lag time. Anion, but not cation, identity influences the rate of IAPP amyloid formation to different extents even in the same ionic strength (40). In addition, IAPP aggregation apparently showed a pH-dependent manner, and the protonation states of His 18 and the N-terminus were considered to be responsible for the effects (41). To validate our observation of acceleration effect caused by glycation, we also compared IAPP and AGE-IAPP aggregation at low pH (Fig. 2 *b*). As expected, we found that the low pH (pH 4.0) environment significantly suppressed the aggregation of IAPP, which agrees with previous results. Although AGE-IAPP also showed retarded kinetics at pH 4.0, a clear 50 h lag time can be recognized from a sigmoidal curve of AGE-IAPP amyloid formation, indicating that the modification by

glycation does enhance the amyloidogenicity of IAPP. To confirm the formation of amyloid fibrils by both peptides, the ThT end products incubated in 10 mM Tris (pH 7.4) were collected and subjected to TEM. Under the resolution provided by TEM, both peptides were found to form typical long and unbranched fibrils, and the fibril morphologies of AGE-IAPP were very similar to IAPP, suggesting that glycation on the first residue did not significantly change the fibril structure. Although the fibril structure of IAPP has not been totally decrypted, with the assistance of solid-state NMR and other structure studies, IAPP fibrils are shown to be composed of two columns of IAPP monomers that adopt a U-shaped structure and contain two $\beta$-stands (42,43). However, the first seven amino acids were not in the region of the ordered $\beta$-sheet structure, it is understandable that the fibril structure of AGE-IAPP could remain the same as IAPP.

## Glycation promotes the conformational change of IAPP from random coil to $\beta$-sheet structure

IAPP is an intrinsically disordered protein. In general, freshly prepared IAPP in aqueous solution exhibits primarily random coil structure with transient helical conformation (44). The conformation of IAPP would gradually convert to $\beta$-sheets along with protein aggregation. Therefore, we applied CD to record the secondary structure changes of both IAPP and AGE-IAPP peptides. As shown in Fig. 3 *a*, freshly dissolved IAPP first displayed a random coil structure and formed typical $\beta$-sheet conformation after 24 h of incubation at pH 7.4. However, the CD spectra of AGE-IAPP showed different signal profiles compared to IAPP. After 12 h incubation, AGE-IAPP already exhibited a combination of 50% random coil and 46% $\beta$-sheet structures, which was estimated by BeStSel (45) (Fig. 3 *b*). After that, the CD signals gradually disappeared. We speculated that the loss of CD signals may be due to the formation of insoluble fibrillar aggregates. TEM images for IAPP and AGE-IAPP at 24, 36, and 48 h were taken to validate this phenomenon (Fig. S1). Indeed, at 24 h, AGE-IAPP has been found to form mature fibrils. In comparison with IAPP, AGE-IAPP takes much less time to form $\beta$-sheet structures, indicating that glycation induces conformation changes of IAPP.

## Glycation induces the formation of high-molecular-weight IAPP oligomers

Most histological studies have shown that deposits of islet amyloid are extracellular, but the initial occurrence site of islet amyloid formation is not known. However, both intracellular and extracellular IAPP oligomers were shown to cause the death of pancreatic $\beta$ cells (11,46). Understanding the properties of toxic IAPP oligomers is therefore important. Most observations were in agreement with the concept

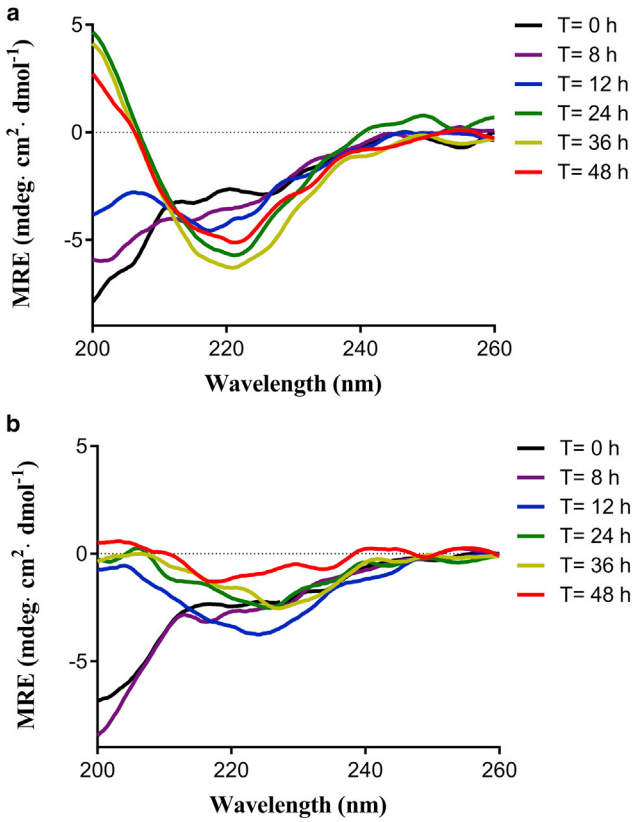


FIGURE 3 Effect of glycation on conformational change of IAPP. Time-course CD spectra of IAPP (*a*) and AGE-IAPP (*b*) are shown. Peptides were incubated in 10 mM Tris buffer (pH 7.4) with mild agitation (shaken 60 s per hour at 500 rpm). The spectra were collected from 200 to 260 nm after incubation for 0, 8, 12, 24, 36, and 48 h. To see this figure in color, go online.

that IAPP oligomers are preamyloid lag-phase intermediates and ThT signal negative. More recently, IAPP oligomers, but not IAPP fibrils, are suggested to mediate $\beta$-cell toxicity through the binding of the receptor for advanced glycation end products (RAGE) to activate the proinflammatory gene (47). RAGE can bind AGEs, including glycoprotein modified through the Millard reaction. Generally, in diabetes and other chronic diseases, the level of RAGE is usually found to be elevated (21). Although it is not known whether RAGE shows a preference for glycated IAPP oligomers, here, we first characterized the oligomer species formed by IAPP and AGE-IAPP in the early stage of aggregation. The relative abundance of monomeric or oligomeric species of cross-linked IAPP was revealed by SDS-PAGE with Western blotting. Samples were separated using a 13.5% Tris-Tricine gel, which can provide better identification for protein size under 100 kDa. Fig. 4 showed that freshly prepared IAPP and AGE-IAPP samples already exhibited different protein molecular weight distribution. The dominant species of IAPP were monomers, with some oligomers between 15 and 25 kDa, whereas the monomeric AGE-IAPP was not observed. Faint dimer and trimer

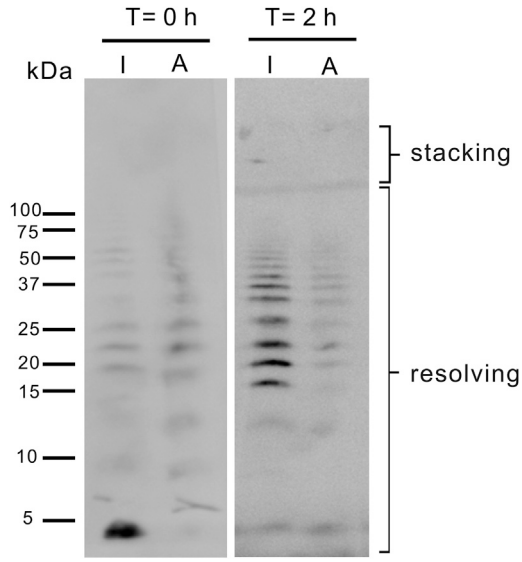


FIGURE 4 Glycation promotes the formation of oligomer species. 32 $\mu$M IAPP and AGE-IAPP were incubated for 0 and 2 h, fixed by photo-induced cross-linking of unmodified protein, and revealed by Western blot to analyze oligomer distribution. I represents IAPP, and A represents AGE-IAPP.

bands were revealed, and tetramers, pentamers, and hexamers are the most populated species of AGE-IAPP. After 2 h incubation, IAPP also formed small oligomers in the 15–50 kDa range. However, the signal of protein bands for AGE-IAPP was reduced. We conjectured that it may form larger aggregates that are not soluble in solution for gel separation. Later, we applied the similar approach using a 4–20% gradient Tris-glycine gel to reveal the protein size of AGE-IAPP. A smeared band range from 75 to 250 kDa was shown, suggesting that glycation promotes the formation of high-molecular-weight oligomer species (Fig. S1). The cause of formation of higher-molecular-weight species by AGE-IAPP was not clear. However, it may help explain the acceleration effect observed for AGE-IAPP aggregation. IAPP is a positively charged polypeptide in pH 7.4. The glycation modification would change the charge of the amino-acid side chain at position 1 from positive to negative and decrease the net charge of IAPP. Previous studies have showed the decrease of net charge of IAPP does not always promote amyloid formation (48). Therefore, a likely explanation is that a new possible favorable electrostatic interaction may be formed during AGE-IAPP aggregation to overcome unfavorable electrostatic repulsion between cationic peptides in the early stage oligomerization (40).

## AGE-IAPP triggers amyloid formation by IAPP

As mentioned previously, AGE-IAPP formed amyloid fibrils faster than unmodified IAPP and proceeded with faster conformational change from random coil to $\beta$-sheets. Thus, we performed a coassembly experiment to confirm whether the presence of AGE-IAPP can manipulate overall protein aggregation. IAPP was incubated with AGE-IAPP at different ratios from 3:1 to 1:3 (IAPP/AGE-IAPP), and total protein concentration was fixed at 32 $\mu$M. Again, the amyloid formation by peptide mixture was monitored by ThT fluorescence assay. Interestingly, no matter what percentage of AGE-IAPP in the mixture, the kinetic profiles of amyloid formation for conditions containing AGE-IAPP are almost identical to the one of AGE-IAPP alone (Fig. 5). The lag times of protein mixture are similar to the lag time of AGE-IAPP but significantly shorter than IAPP alone. The final ThT intensities of all conditions measured during reaction plateau are statistically similar. We also performed the experiment with a very low molar ratio of AGE-IAPP. Only 10% of AGE-IAPP is needed in mixture to see the acceleration effect (Fig. S3). These data suggested that AGE-IAPP can interact with IAPP and boost the aggregation of IAPP. Even though the details of the conformations of IAPP during this conversion are poorly understood, several models have been proposed for the early stage of nucleation. For example, IAPP was found to form a helix structure between residue 5 and 20 in aqueous buffer and associate with other helical peptide chains in a manner like the formation of coiled-coil motif (44,49,50). On the other hand, data derived from ion-mobility spectrometry-mass spectrometry assisted with molecular dynamic modeling suggested that IAPP dimers were formed by two side-by-side IAPP monomers, which may adopt the $\beta$-hairpin structure (51). More recently, a 2D-IR study reported that IAPP would first convert to ordered $\beta$-sheet oligomers, including FGAIL residues before amyloid growth (52). Surprisingly, none of them have been discussing the role of residues within the N-terminal regions. However, a mutational study done by Bitan's group clearly showed that K1 would contribute to IAPP self-assembly: an N-terminally truncated IAPP analog, $IAPP_{2-37}$, exhibited a much slower nucleation rate and much weaker ThT final intensity compared to wild-type IAPP (53). When IAPP is glycated by glyoxal on Lys the electronic property of this residue would completely change from positive charge to negative charge in

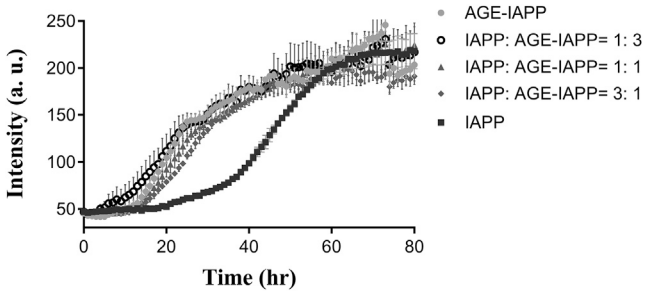


FIGURE 5 Glycation reduces lag time of IAPP aggregation. ThT fluorescence kinetics are shown for AGE-IAPP (*solid circle*); IAPP and AGE-IAPP in a ratio of 1:3 (*open circle*), 1:1 (*triangle*), or 3:1 (*diamond*); and IAPP (*square*). The total peptide concentration was fixed at 32 $\mu$M for each condition. The kinetic experiments were performed in duplicate.

physiological pH environment and also alter the pI value of IAPP. After modification, the pI value of AGE-IAPP is ~6.8, which is close to the pH of the working buffer. The hydrophobic effect would become a more significant attractive force among them. However, IAPP has not been shown that the rate of aggregation does not correlate on the net change of the peptide (48). Though we do not know yet how the aggregation was prompted by introducing of negative charge in the first residue, we speculated that the negatively charged side chain of AGE-IAPP would interact with unmodified IAPP through electrostatic interaction and process a faster aggregation pathway.

## AGE-IAPP fibrils can cross-seed amyloid formation by IAPP

From TEM images, we found that the morphologies of fibrils formed by IAPP and AGE fibrils are quite similar under an optimal resolution of the microscope. Therefore, we attempted to explore more details about the structural similarity between IAPP fibrils and AGE-IAPP fibrils by seeding experiments and tested the potential of AGE-IAPP fibrils in cross-seeding IAPP monomers. In general, preformed amyloid fibrils can act as seeds to induce quick growth of mature fibrils from protein monomers (29,54). Effective seeding usually can be observed from a bypass of lag time during aggregation, when fibrils serve as an appropriate template for their own monomers. A difference in the structure of fibrils would normally affect seeding efficiency (55). Here, the ThT assays were also applied in the seeding experiment to monitor the process of aggregation. First of all, we prepared IAPP fibrils to seed IAPP and AGE-IAPP monomers (Fig. 6 *a*). Consistent with previous studies, 10% IAPP fibrils (in its monomeric unit) can successfully seed amyloid formation by IAPP monomers, resulting in a quick increase of ThT intensity without an obvious lag time. Similar phenomena were also observed when IAPP fibrils were present at the beginning of AGE-IAPP aggregation. Afterward, we used AGE-IAPP fibrils as seeds in seeding both peptides (Fig. 6 *b*). Compared with unseeded reactions, IAPP and AGE-IAPP both formed amyloid fibrils much faster in the presence of AGE-IAPP fibrils, suggesting that both peptides can be seeded by AGE-IAPP fibrils. Our results clearly show that the fibril structure of AGE-IAPP is very similar to that of IAPP. The glycation did not largely change the IAPP fibril morphologies. Additionally, it is worth noting that AGE-IAPP exhibited a faster elongation rate than IAPP in both conditions. We demonstrated here that glycation not only shortened the time of IAPP to form active nucleus but also increased the rate of fibril growth.

## AGE-IAPP maintains the ability to interact with model lipid vesicles and exhibits cytotoxicity to MIN6 cells

IAPP is a hormone produced from $\beta$-cells in the islets of Langerhans and formation of islet amyloid has been shown to induce apoptosis in the cell culture (5). Several mechanisms have been proposed to describe how this small peptide contributes to cell toxicity; however, so far, it has no clear conclusion yet. In some in vitro studies, IAPP was shown to be capable of damaging the cell membrane, and the toxic properties of IAPP may be due to its interaction with the membrane surface (9,10,56). Electrostatic interactions were first considered to play a role in directing positive-charged IAPP to make contact with the negative membrane surface (57,58). Indeed, IAPP was shown to be more effective in inducing leakage of membrane containing a high percentage of anionic lipids. In our study, glycation apparently changes the electronic properties of the N-terminus of IAPP. Therefore, we next examined the level of IAPP or AGE-IAPP induced membrane leakages because membrane and IAPP interactions have been proposed to contribute to IAPP toxicity. We characterized the permeability of the membrane vesicles (composed of 60 mol% DMPC, 20 mol% DMPG, and 20 mol% cholesterol; Fig. 7 *a*) by detecting the fluorescence of carboxyfluorescein, whose fluorescence is self-quenched when it was

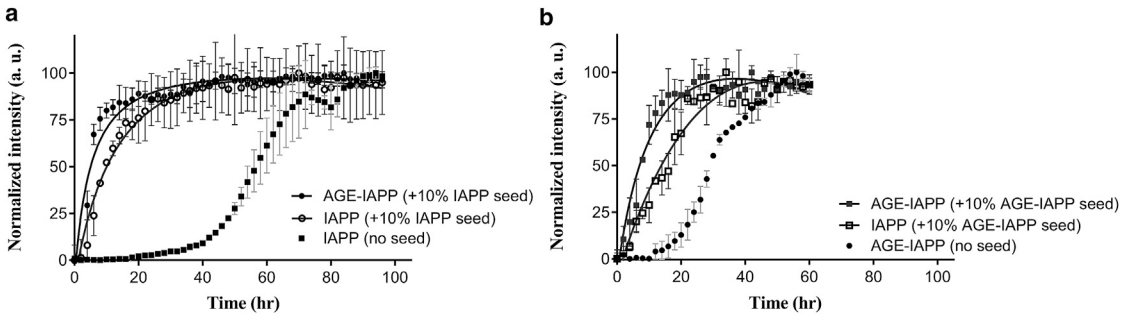


FIGURE 6 Preformed AGE-IAPP fibrils can seed amyloid formation by IAPP. (*a*) Aggregation of IAPP (*open circle*) and AGE-IAPP (*solid circle*) in the presence of 10% IAPP seeds (in monomeric unit) were monitored by ThT assays. The curve with square symbol represents unseeded IAPP (*b*) Aggregation of IAPP (*open square*) and AGE-IAPP (*solid square*) in the presence of 10% AGE-IAPP seeds (in monomeric unit) was monitored by ThT assays. The curve depicted with black dots represents unseeded AGE-IAPP. The final intensity was normalized at the spectral maxima. Experiments were conducted with 32 $\mu$M peptide in 10 mM Tris buffer (pH 7.4) at 25°C without further agitation.

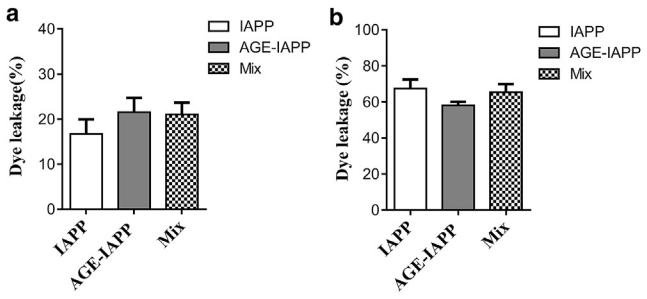


FIGURE 7 The level of membrane leakage induced by IAPP, AGE-IAPP, and protein mixtures including IAPP and AGE-IAPP at a 1:1 ratio. Experiments done in duplicate were performed in 20 mM Tris buffer with 100 mM NaCl at 25°C. Peptide (12 $\mu$M)/lipid ratio was fixed at 1:100. (*a*) The membrane composition is 60 mol% DMPC, 20 mol% DMPG, and 20 mol% cholesterol. (*b*) The membrane composition is 49 mol% POPC, 21 mol% POPS, and 30 mol% cholesterol.

encapsulated within vesicles at higher concentration. Peptide-induced leakage allows the dye to restore its fluorescence when it spread out from vesicles. After 8 h incubation, enough time to reach a signal plateau, we found that IAPP led to a 17% change in fluorescence, which is normalized to an intensity change in the presence of 1% Triton X-100. Both AGE-IAPP and peptide mixtures containing IAPP and AGE-IAPP at a 1:1 ratio showed a 21% fluorescence change. On the other hand, because it is known that lipid composition also may affect IAPP-membrane interactions (58), we prepared another membrane vesicle containing 49 mol% POPC, 21 mol% POPS, and 30 mol% cholesterol. The results in Fig. 7 *b* showed that the leakage level reached 60% for IAPP, AGE-IAPP, and peptide mixtures, and that is very different from the level observed in previous condition. However, there is no significant difference between IAPP and AGE-IAPP in interacting synthetic membranes. Overall, the data suggest that AGE-IAPP maintains the ability to disrupt the integrity of the membrane. In addition, we examined the biological impacts of AGE-IAPP and protein mixture. The cytotoxicity of IAPP, AGE-IAPP, and peptide mixture with a share ratio of 1:1 was evaluated using pancreatic $\beta$-cell lines MIN6 (Fig. 8). We tested the effects of 1, 8, 16, 32, and 64 $\mu$M peptides on cell viability after 4 and 24 h of incubation of the peptides with the cells. At 4 h, there was no acute toxicity observed. A further decrease in toxicity was found for peptides with higher concentrations after 24 h incubation.

## CONCLUSIONS

Formation of islet amyloid is highly associated with the development of T2D and has also been proposed to cause $\beta$-cell dysfunction and death. IAPP is a major component of islet amyloid deposits. Use of an anti-AGE antibody first identified that AGEs colocalize with regions that are immunoreactive to IAPP in the human islet. Later, further immunologic evidence indicated that IAPP was modified in amyloidogenesis, and nonenzymatic glycation modification was postulated to alter antibody reorganization. Protein glycation leads to the addition of sugar residues to amino groups of proteins and forms AGEs. Several previous reports showed that AGEs are present not only in brain tissue of patients with AD but also in amyloid deposits formed by tau protein, $\beta_2$-microglobulin, prions, transthyretin, etc. However, the effect of glycation on these proteins does not seem to be identical. The molecular basis of this modulation is still poorly understood. In this study, we describe how protein glycation affects the properties of IAPP in terms of the aggregation process, fibril morphology, the rate of fibril elongation, interaction with lipid vesicles, and cytotoxicity. We find that glycation by glyoxal significantly promotes IAPP to form high-molecular-weight species and its structural conversion from random coil to $\beta$-sheets. From seeding experiments, AGE-IAPP also was found to exhibit faster elongation rate. We believed that this is why AGE-IAPP was observed to aggregate much faster than normal IAPP. Glycation may not greatly change the fibril structure of IAPP because IAPP can be seeded by a

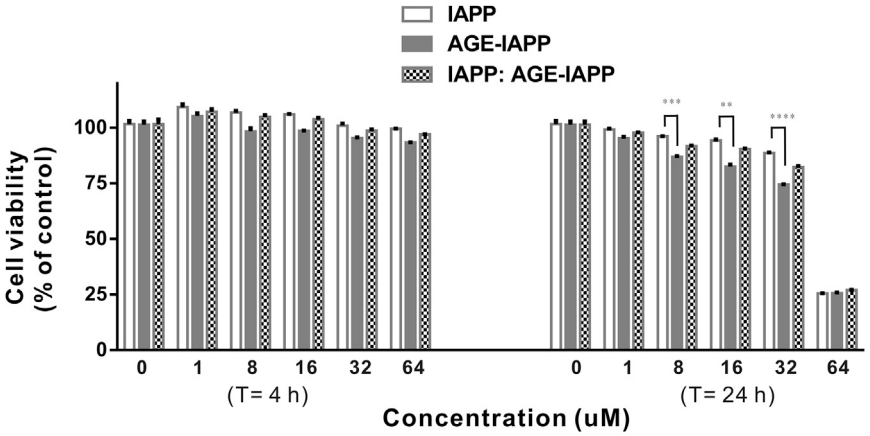


FIGURE 8 Cell viability of MIN6 cells following incubation with various concentration of IAPP, AGE-IAPP, and protein mixtures including IAPP and AGE-IAPP at a 1:1 ratio. MIN6 pancreatic $\beta$ cells were treated with various concentrations of IAPP, AGE-IAPP, and IAPP:AGE-IAPP = 1:1 for 4 or 24 h before cell viability was measured. Cell viability was determined by Alamar Blue assay and compared to that of cells treated with vehicle (100% cell viability). The statistical significance between IAPP and AGE-IAPP was indicated by one-way ANOVA (****$p < 0.0001$; ***$p < 0.001$; **$p < 0.005$).

relatively small amount of preformed AGE-IAPP fibrils and quickly formed amyloid fibrils without apparent delay. Our investigation shown here aimed to provide a general model for amyloid formation under hyperglycemia. Although it is not known whether this type of modification occurs before protein aggregation or after fibril formation in vivo, our work shown here and previous work done by Bucala et al. can represent two different situations of protein glycation. Protein glycation is a complicated process, and it is not possible to simply deduce its effect by our methods or methods in other studies. However, we hope to provide a possible link among hyperglycemia, diabetes, and IAPP. That would help us in understanding of amyloidosis. We propose that glycation would enhance the production of IAPP oligomers, which are generally considered toxic species, and our data also confirmed that AGE-IAPP is cytotoxic. The presence of glycated IAPP could induce normal IAPP to proceed aggregation pathway. It would be very important to develop new methods in preventing glycation or consider glycated IAPP, but not native IAPP, as a target protein for inhibitor design if this hypothesis is true. On the other hand, it will be very interesting to deduce the role of Lys in IAPP amyloid formation; hence, further studies are being conducted in the lab to contribute our understanding of the mechanism of fibril formation.

## SUPPORTING MATERIAL

Supporting Material can be found online at https://doi.org/10.1016/j.bpj.2019.05.013.

## AUTHOR CONTRIBUTIONS

L.-H.T., Y.-W.C., M.-H.W., and Y.-H.H. conducted experiments. L.-H.T. provided concepts, analyzed the data, and wrote the manuscript.

## ACKNOWLEDGMENTS

We thank Ms. Ya-Yun Yang from the instrumentation center of the National Taiwan University and Wei-Xuan Teh for the assistance in TEM experiments.

The work was supported by Ministry of Science and Technology, Taiwan (MOST 105-2133-M-003-014-MY2).

## REFERENCES

1. Westermark, P. 1972. Quantitative studies on amyloid in the islets of Langerhans. *Ups. J. Med. Sci.* 77:91–94.
2. Cooper, G. J., A. C. Willis, …, K. B. Reid. 1987. Purification and characterization of a peptide from amyloid-rich pancreases of type 2 diabetic patients. *Proc. Natl. Acad. Sci. USA.* 84:8628–8632.
3. Maloy, A. L., D. S. Longnecker, and E. R. Greenberg. 1981. The relation of islet amyloid to the clinical type of diabetes. *Hum. Pathol.* 12:917–922.
4. Mosselman, S., J. W. Höppener, …, H. S. Jansz. 1988. Islet amyloid polypeptide: identification and chromosomal localization of the human gene. *FEBS Lett.* 239:227–232.
5. Cao, P., P. Marek, …, D. P. Raleigh. 2013. Islet amyloid: from fundamental biophysics to mechanisms of cytotoxicity. *FEBS Lett.* 587:1106–1118.
6. Wang, J., J. Xu, …, C. B. Verchere. 2001. The prohormone convertase enzyme 2 (PC2) is essential for processing pro-islet amyloid polypeptide at the NH2-terminal cleavage site. *Diabetes.* 50:534–539.
7. Marzban, L., G. Trigo-Gonzalez, …, C. B. Verchere. 2004. Role of beta-cell prohormone convertase (PC)1/3 in processing of pro-islet amyloid polypeptide. *Diabetes.* 53:141–148.
8. Marzban, L., G. Soukhatcheva, and C. B. Verchere. 2005. Role of carboxypeptidase E in processing of pro-islet amyloid polypeptide in beta-cells. *Endocrinology.* 146:1808–1817.
9. Weise, K., D. Radovan, …, R. Winter. 2010. Interaction of hIAPP with model raft membranes and pancreatic beta-cells: cytotoxicity of hIAPP oligomers. *Chembiochem.* 11:1280–1290.
10. Janson, J., R. H. Ashley, …, P. C. Butler. 1999. The mechanism of islet amyloid polypeptide toxicity is membrane disruption by intermediate-sized toxic amyloid particles. *Diabetes.* 48:491–498.
11. Zraika, S., R. L. Hull, …, S. E. Kahn. 2010. Toxic oligomers and islet beta cell death: guilty by association or convicted by circumstantial evidence? *Diabetologia.* 53:1046–1056.
12. Kumar, S., and J. Walter. 2011. Phosphorylation of amyloid beta (Aβ) peptides - a trigger for formation of toxic aggregates in Alzheimer's disease. *Aging (Albany N.Y.).* 3:803–812.
13. Cao, P., A. Abedini, …, D. P. Raleigh. 2013. Islet amyloid polypeptide toxicity and membrane interactions. *Proc. Natl. Acad. Sci. USA.* 110:19279–19284.
14. Costes, S., R. Langen, …, P. C. Butler. 2013. β-Cell failure in type 2 diabetes: a case of asking too much of too few? *Diabetes.* 62:327–335.
15. Nguyen, P. T., X. Zottig, …, S. Bourgault. 2017. Role of site-specific asparagine deamidation in islet amyloid polypeptide amyloidogenesis: key contributions of residues 14 and 21. *Biochemistry.* 56:3808–3817.
16. Dunkelberger, E. B., L. E. Buchanan, …, M. T. Zanni. 2012. Deamidation accelerates amyloid formation and alters amylin fiber structure. *J. Am. Chem. Soc.* 134:12658–12667.
17. Abedini, A., and D. P. Raleigh. 2006. Destabilization of human IAPP amyloid fibrils by proline mutations outside of the putative amyloidogenic domain: is there a critical amyloidogenic domain in human IAPP? *J. Mol. Biol.* 355:274–281.
18. Koo, B. W., J. A. Hebda, and A. D. Miranker. 2008. Amide inequivalence in the fibrillar assembly of islet amyloid polypeptide. *Protein Eng. Des. Sel.* 21:147–154.
19. Tu, L. H., and D. P. Raleigh. 2013. Role of aromatic interactions in amyloid formation by islet amyloid polypeptide. *Biochemistry.* 52:333–342.
20. Ulrich, P., and A. Cerami. 2001. Protein glycation, diabetes, and aging. *Recent Prog. Horm. Res.* 56:1–21.
21. Ahmed, N. 2005. Advanced glycation endproducts–role in pathology of diabetic complications. *Diabetes Res. Clin. Pract.* 67:3–21.
22. Singh, V. P., A. Bali, …, A. S. Jaggi. 2014. Advanced glycation end products and diabetic complications. *Korean J. Physiol. Pharmacol.* 18:1–14.
23. Delgado-Andrade, C. 2016. Carboxymethyl-lysine: thirty years of investigation in the field of AGE formation. *Food Funct.* 7:46–57.
24. Vitek, M. P., K. Bhattacharya, …, A. Cerami. 1994. Advanced glycation end products contribute to amyloidosis in Alzheimer disease. *Proc. Natl. Acad. Sci. USA.* 91:4766–4770.
25. Iannuzzi, C., G. Irace, and I. Sirangelo. 2014. Differential effects of glycation on protein aggregation and amyloid formation. *Front. Mol. Biosci.* 1:9.

26. Iannuzzi, C., M. Borriello, …, I. Sirangelo. 2016. D-ribose-glycation of insulin prevents amyloid aggregation and produces cytotoxic adducts. *Biochim. Biophys. Acta.* 1862:93–104.

27. Liu, K., Y. Liu, …, H. Qing. 2016. Glycation alter the process of Tau phosphorylation to change Tau isoforms aggregation property. *Biochim. Biophys. Acta.* 1862:192–201.

28. Vicente Miranda, H., E. M. Szego, …, T. F. Outeiro. 2017. Glycation potentiates α-synuclein-associated neurodegeneration in synucleinopathies. *Brain.* 140:1399–1419.

29. Kapurniotu, A., J. Bernhagen, …, R. Bucala. 1998. Contribution of advanced glycosylation to the amyloidogenicity of islet amyloid polypeptide. *Eur. J. Biochem.* 251:208–216.

30. Ma, Z., P. Westermark, and G. T. Westermark. 2000. Amyloid in human islets of Langerhans: immunologic evidence that islet amyloid polypeptide is modified in amyloidogenesis. *Pancreas.* 21:212–218.

31. Abedini, A., and D. P. Raleigh. 2005. Incorporation of pseudoproline derivatives allows the facile synthesis of human IAPP, a highly amyloidogenic and aggregation-prone polypeptide. *Org. Lett.* 7:693–696.

32. Chang, H. Y., S. L. Chen, …, Y. W. Chen. 2017. Selective serotonin reuptake inhibitor, fluoxetine, impairs E-cadherin-mediated cell adhesion and alters calcium homeostasis in pancreatic beta cells. *Sci. Rep.* 7:3515.

33. Thornalley, P. J., A. Langborg, and H. S. Minhas. 1999. Formation of glyoxal, methylglyoxal and 3-deoxyglucosone in the glycation of proteins by glucose. *Biochem. J.* 344:109–116.

34. Iannuzzi, C., G. Irace, and I. Sirangelo. 2014. Differential effects of glycation on protein aggregation and amyloid formation. *Front. Mol. Biosci.* 1:9.

35. Münch, G., S. Mayer, …, A. M. Cunningham. 1997. Influence of advanced glycation end-products and AGE-inhibitors on nucleation-dependent polymerization of beta-amyloid peptide. *Biochim. Biophys. Acta.* 1360:17–29.

36. Jana, A. K., K. B. Batkulwar, …, N. Sengupta. 2016. Glycation induces conformational changes in the amyloid-β peptide and enhances its aggregation propensity: molecular insights. *Phys. Chem. Chem. Phys.* 18:31446–31458.

37. Li, X. H., L. L. Du, …, X. W. Zhou. 2013. Glycation exacerbates the neuronal toxicity of β-amyloid. *Cell Death Dis.* 4:e673.

38. Oliveira, L. M., A. Lages, …, A. Quintas. 2011. Insulin glycation by methylglyoxal results in native-like aggregation and inhibition of fibril formation. *BMC Biochem.* 12:41.

39. Ban, T., D. Hamada, …, Y. Goto. 2003. Direct observation of amyloid fibril growth monitored by thioflavin T fluorescence. *J. Biol. Chem.* 278:16462–16465.

40. Marek, P. J., V. Patsalo, …, D. P. Raleigh. 2012. Ionic strength effects on amyloid formation by amylin are a complicated interplay among Debye screening, ion selectivity, and Hofmeister effects. *Biochemistry.* 51:8478–8490.

41. Abedini, A., and D. P. Raleigh. 2005. The role of His-18 in amyloid formation by human islet amyloid polypeptide. *Biochemistry.* 44:16284–16291.

42. Luca, S., W. M. Yau, …, R. Tycko. 2007. Peptide conformation and supramolecular organization in amylin fibrils: constraints from solid-state NMR. *Biochemistry.* 46:13505–13522.

43. Wiltzius, J. J., S. A. Sievers, …, D. Eisenberg. 2008. Atomic structure of the cross-beta spine of islet amyloid polypeptide (amylin). *Protein Sci.* 17:1467–1474.

44. Williamson, J. A., and A. D. Miranker. 2007. Direct detection of transient alpha-helical states in islet amyloid polypeptide. *Protein Sci.* 16:110–117.

45. Micsonai, A., F. Wien, …, J. Kardos. 2018. BeStSel: a web server for accurate protein secondary structure prediction and fold recognition from the circular dichroism spectra. *Nucleic Acids Res.* 46:W315–W322.

46. Meier, J. J., R. Kayed, …, P. C. Butler. 2006. Inhibition of human IAPP fibril formation does not prevent beta-cell death: evidence for distinct actions of oligomers and fibrils of human IAPP. *Am. J. Physiol. Endocrinol. Metab.* 291:E1317–E1324.

47. Abedini, A., P. Cao, …, A. M. Schmidt. 2018. RAGE binds preamyloid IAPP intermediates and mediates pancreatic β cell proteotoxicity. *J. Clin. Invest.* 128:682–698.

48. Tu, L. H., A. L. Serrano, …, D. P. Raleigh. 2014. Mutational analysis of preamyloid intermediates: the role of his-tyr interactions in islet amyloid formation. *Biophys. J.* 106:1520–1527.

49. Abedini, A., and D. P. Raleigh. 2009. A critical assessment of the role of helical intermediates in amyloid formation by natively unfolded proteins and polypeptides. *Protein Eng. Des. Sel.* 22:453–459.

50. Wiltzius, J. J., S. A. Sievers, …, D. Eisenberg. 2009. Atomic structures of IAPP (amylin) fusions suggest a mechanism for fibrillation and the role of insulin in the process. *Protein Sci.* 18:1521–1530.

51. Dupuis, N. F., C. Wu, …, M. T. Bowers. 2011. The amyloid formation mechanism in human IAPP: dimers have β-strand monomer-monomer interfaces. *J. Am. Chem. Soc.* 133:7240–7243.

52. Serrano, A. L., J. P. Lomont, …, M. T. Zanni. 2017. A free energy barrier caused by the refolding of an oligomeric intermediate controls the lag time of amyloid formation by hIAPP. *J. Am. Chem. Soc.* 139:16748–16758.

53. Lopes, D. H., A. Attar, …, G. Bitan. 2015. Molecular tweezers inhibit islet amyloid polypeptide assembly and toxicity by a new mechanism. *ACS Chem. Biol.* 10:1555–1569.

54. Krebs, M. R., L. A. Morozova-Roche, …, C. M. Dobson. 2004. Observation of sequence specificity in the seeding of protein amyloid fibrils. *Protein Sci.* 13:1933–1938.

55. O'Nuallain, B., A. D. Williams, …, R. Wetzel. 2004. Seeding specificity in amyloid growth induced by heterologous fibrils. *J. Biol. Chem.* 279:17490–17499.

56. Khemtémourian, L., J. A. Killian, …, M. F. Engel. 2008. Recent insights in islet amyloid polypeptide-induced membrane disruption and its role in beta-cell death in type 2 diabetes mellitus. *Exp. Diabetes Res.* 2008:421287.

57. Nanga, R. P., J. R. Brender, …, A. Ramamoorthy. 2011. Structure and membrane orientation of IAPP in its natively amidated form at physiological pH in a membrane environment. *Biochim. Biophys. Acta.* 1808:2337–2342.

58. Zhang, X., J. R. St Clair, …, D. P. Raleigh. 2017. Islet amyloid polypeptide membrane interactions: effects of membrane composition. *Biochemistry.* 56:376–390.

**Biophysical Journal, Volume *116***

## Supplemental Information

# Protein Glycation by Glyoxal Promotes Amyloid Formation by Islet Amyloid Polypeptide

**Yi-Hsuan Hsu, Yun-Wen Chen, Meng-Hsin Wu, and Ling-Hsien Tu**

# Supporting Information for

## Protein glycation by glyoxal promotes amyloid formation by islet amyloid polypeptide

Yi-Hsuan Hsu†, Yun-Wen Chen‡, Meng-Hsien Wu†, and Ling-Hsien Tu†*

†Department of Chemistry, National Taiwan Normal University, Taipei 116, Taiwan

‡Department of Pharmacology, College of Medicine, National Cheng Kung University, Tainan 701, Taiwan.

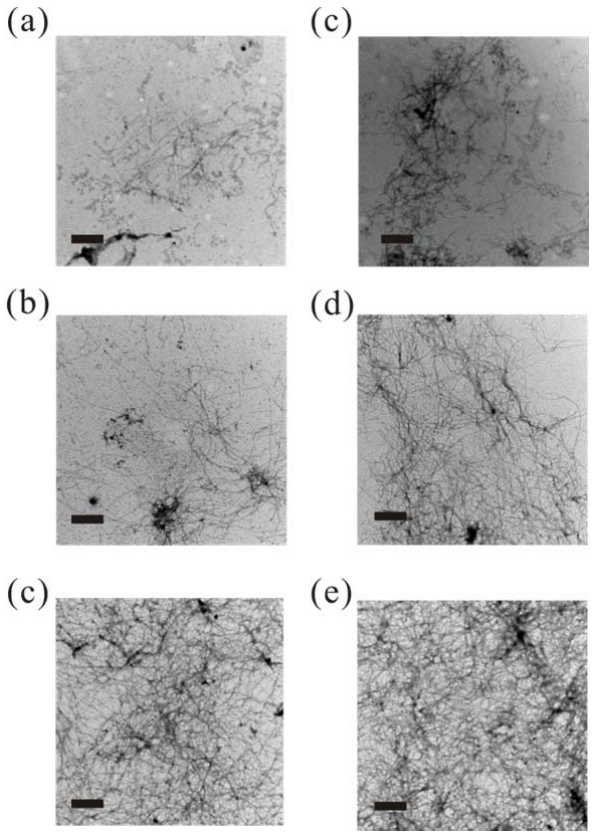


**Figure S1**: (a-c) TEM images for IAPP samples which were incubated for 24, 36, and 48 h. (c-d) TEM images for AGE-IAPP samples which were incubated for 24, 36, and 48 h. Protein samples were prepared in the same condition as CD experiments. The scale bar represents 500 nm.

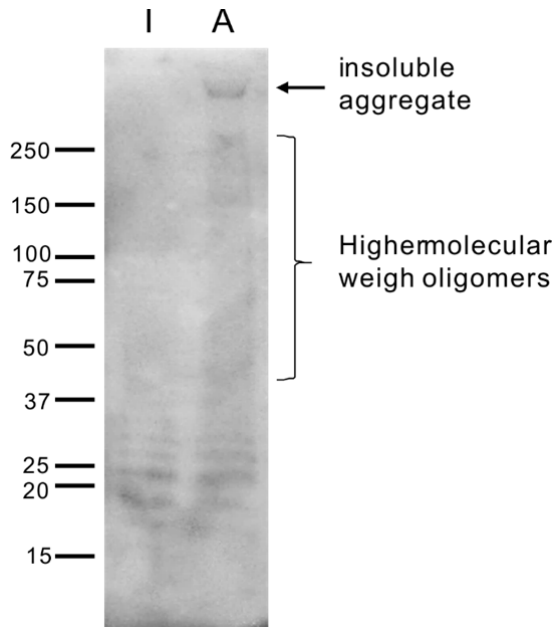


**Figure S2**: Oligomer distribution of unlinked IAPP and AGE-IAPP revealed by 4-20% gradient Tris-glycine gel and probed by IAPP antibody R10/99 after 2 h incubation. Protein samples were prepared at 32 μM in pH 7.4, 10 mM Tris buffer at 25 $^{o}$C. I represents IAPP and A represents AGE-IAPP.

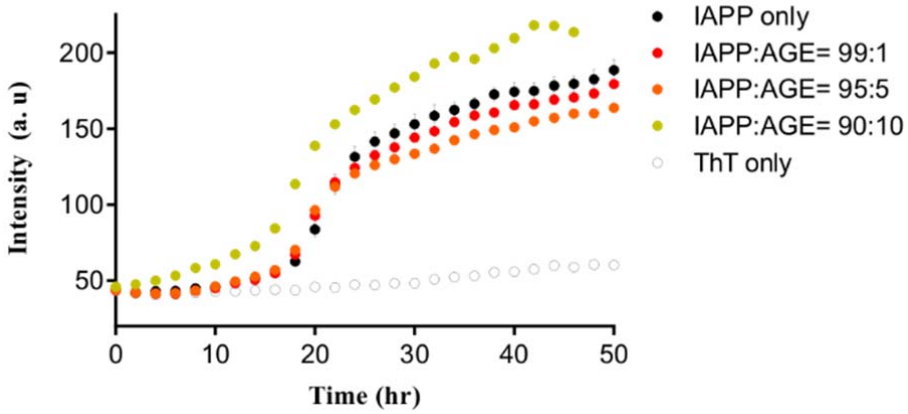


**Figure S3**. ThT fluorescence kinetics were shown for IAPP (black), IAPP and AGE-IAPP in a ratio of 99: 1 (red), 95: 5 (orange), and 90: 10 (dark yellow). The total peptide concentration was fixed at 32 μM for each condition. The kinetic experiments were performed in duplicate.